9-2023

Carbohydrates generated via hot water as catalyst for CO2 reduction reaction

Yang Yang

Heng Zhong

Jiong Cheng

Yun Hang Hu

Richard Lee Smith Jr

See next page for additional authors

Authors

Yang Yang, Heng Zhong, Jiong Cheng, Yun Hang Hu, Richard Lee Smith Jr, and Fangming Jin

Next Energy 1 (2023) 100037

Contents lists available at ScienceDirect

Next Energy

journal homepage: www.sciencedirect.com/journal/next-energy

Research article

Carbohydrates generated via hot water as catalyst for CO_2 reduction reaction

Yang Yang[a], Heng Zhong[a], Jiong Cheng[a], Yun Hang Hu[c], Richard Lee Smith Jr[d], Fangming Jin[a,b,*]

[a] School of Environmental Science and Engineering, Shanghai Jiao Tong University, Shanghai 200240, China
[b] State Key Laboratory of Metal Matrix Composites, Shanghai Jiao Tong University, Shanghai 200092, China
[c] Department of Materials Science and Engineering, Michigan Technological University, Houghton, Michigan 49931, United States
[d] Graduate School of Environmental Studies, Tohoku University, Aramaki Aza Aoba 468-1, Aoba-ku, Sendai 980-8572, Japan

ARTICLE INFO

Keywords:
CO_2 reduction
Biomass
Hydrothermal
Abiotic synthesis
Green hydrogen
Mechanism

ABSTRACT

Combining terrestrial biomass with submarine-type hydrothermal environments for CO_2 reduction is a possible approach for realizing new energies while achieving sustainable circulation of carbon. Herein, carbohydrate-enabled CO_2 reduction based on $NaHCO_3$ conversion to formate revealed that hydrothermal environments facilitated direct hydrogen transfer from carbohydrates (glucose, cellulose) to CO_2/$NaHCO_3$ with hot water (250–300 °C, 5–20 MPa) acting as homogeneous catalyst in absence of any conventional catalysts giving CO_2/$NaHCO_3$ reduction efficiencies as high as 76% for cellulose. Time-resolved operando hydrothermal DRIFTS spectra of glycolaldehyde in hot water (250 °C, autogenous pressure) verified that water catalyzed $NaHCO_3$ reduction by converting the -CHO group in the carbohydrate to its hydrated state as $-CH(OH)_2$, which enabled $NaHCO_3$ reduction by direct hydrogen transfer and that the ratio of hydrogen transfer from water:-glycolaldehyde for $NaHCO_3$ reduction was about 13:87 on an atom basis. For cellulose exploited as energy input, a greater than 3.4% solar-to-formate efficiency can be theoretically attained, which is unprecedented compared with present literature values. These findings provide basic data for future studies on biomass-enabled CO_2 reduction and broaden the scope of hydrothermal chemistry for developing net-zero emission processes.

Introduction

Humanity's voracious consumption of fossil fuels is leading to growing atmospheric CO_2 concentrations with corresponding threats to the environment. To achieve sustainability, CO_2 reduction technologies must be developed that have two requirements: net-zero emissions and high efficiency. [1–3] The first requirement could be met by photo-catalytic CO_2 conversion systems, [4,5] however, direct solar-to-fuel conversion processes have only attained efficiencies of less than 1% with noble catalysts, and their general applicability is limited. [6,7] Catalytic hydrogenation can be used for CO_2 reduction with relatively high efficiencies and selectivities, [8,9] but hydrogen used in many proposed schemes is derived from non-renewable fossil fuels, [10,11] posing difficulties in achieving overall net-zero emissions. An integrated system for CO_2 reduction into CH_3OH by combining solar cells, electrolysis of water and CO_2 hydrogenation has been proposed to enhance photo-catalytic CO_2 conversion efficiency, [12] but the chemical steps are complex and the system sustainability still requires development.

Abiotic reduction of CO_2 dissolved in water to form organic molecules initiated by serpentinization in natural H_2-rich alkaline hydrothermal vents has drawn particular interest, [13,14] since it provides favorable conditions for sustainable reduction of carbon compounds fundamental to Earth's carbon cycle. Nature's hydrothermal reduction environments are also believed to have contributed to the origins of life and to the formation of a large proportion of natural petroleum. [15–18] Thus, different ways of reducing CO_2 can be achieved by mimicking geochemically robust hydrothermal vent systems for CO_2 reduction. In the synthesis of abiotic organic molecules in natural hydrothermal systems isolated from solar radiation and power generation without energy input from sunlight, reducing conditions are produced through the reaction of ferrous Fe-bearing oxide and/or sulfide minerals with hot water. [19–21] In simulated geochemical hydrothermal environments, the choice of reductant or reducing energy input is of primary importance for achieving net-zero emissions and efficient CO_2 reduction.

Biomass and bio-related organic compounds can contain highly active and reductive functional groups (-OH, -CHO, $-NH_2$) which afford hydrogen production in hydrothermal environments, [22–26] rendering biochemicals as a viable hydrogen donor source for CO_2 reduction. Since biomass stores solar energy, using it to drive CO_2

* Corresponding author at: School of Environmental Science and Engineering, Shanghai Jiao Tong University, Shanghai 200240, China.
E-mail address: fmjin@sjtu.edu.cn (F. Jin).

https://doi.org/10.1016/j.nxener.2023.100037
Received 30 April 2023; Received in revised form 13 June 2023; Accepted 23 June 2023

reduction offers great potential in the effort to gain net-zero emission reaction systems. Moreover, CO_2 is naturally fixed through photosynthesis in biomass, thus, additional CO_2 reduction with biomass allows double CO_2 fixation. De facto, biomass has been employed as a compensated energy source for CO_2 reduction in electrochemical systems, owing to its much lower theoretical electricity consumption. [27] This kind of consideration conforms to the growing view that sustainability must be included in performance metrics in conversion systems. [28] While substantial progress has been made in developing electrochemical systems, [29–31] many challenges still remain in exploiting biomass energy for its complete oxidation or selective conversion. [32,33].

On the other hand, hydrothermal environments have shown their effectiveness for biomass conversion, particularly in rapid breakage of chemical bonds and chemical transformations. [34,35] For example, continuous reaction systems have been demonstrated for biomass conversions that have maximum treatment capacities of 2 kg h^{-1} of dry biomass for acetic acid production. [36,37] Biomass has intrinsic reactivity to support sustainable CO_2 reduction as can be seen by examples for carbohydrate derivatives such as glucitol and glycerol, and marine biomass as microalgae, [38–40] that show prospects for large-scale implementation of CO_2 reduction systems under hydrothermal conditions. Consequently, detailed mechanisms of reduction reactions in hydrothermal environments becomes imperative, which are not easily elucidated due to the high-temperatures (ca. 250 °C) and high-pressures (5–30 MPa) used. When reduction of CO_2 is the target reaction, specially-prepared noble metal-based catalysts are generally required due to the thermodynamic stability of the CO_2 molecule, [41–43] inevitably limiting practical applications of the catalytic systems. On the other hand, water at conditions of high-temperature and high-pressure, which is referred to as hot water in this work, has many unique properties such as weakened hydrogen bonds and high ion product [44] that enable it to act as a homogeneous catalyst for hydrolysis in hydrothermal environments. Therefore, some key questions of this study can be posed as follows. Can the properties of water be manipulated so as to promote a wide scope of carbohydrate-enabled CO_2 reductions and if so, what are the underlying mechanisms of the hydrogen transfer?

Here, we focus on CO_2 reduction by carbohydrate biomass under hydrothermal conditions and describe mechanisms of CO_2 reduction based on $NaHCO_3$ conversion with carbohydrates in the absence of heterogeneous catalysts and how hydrogen is formed from carbohydrate biomass sources. Based on the elucidated mechanisms in CO_2/$NaHCO_3$/carbohydrate/water systems, CO_2 reduction with direct use of cellulose is studied. Furthermore, considering that carbohydrates store solar energy, an estimation is made for a solar-to-formate conversion efficiency.

Experiments

CO_2/$NaHCO_3$ reduction with carbohydrates

All experiments regarding the reduction of CO_2/$NaHCO_3$ with carbohydrates, with the except of investigations with time-resolved operando hydrothermal infrared methods, were conducted using a series of stainless steel 316 tube reactors (9.525 mm (3/8 in.) o.d., 1 mm wall thickness, 120 mm long) with Swagelok caps as end fittings providing an inner volume of 5.7 mL (detailed schematic in Fig. S1). Typical procedures for the batch experiments were as follows. In one-step experiments, desired amounts of $NaHCO_3$ in solid powder form, glucose (or cellulose) and water were loaded into the reactor which was then sealed and placed into a salt bath preheated to reaction temperature. After a given time, the reactor was removed from the salt bath and immediately immersed in a cold-water bath to terminate the reaction. In two-step experiments, a desired amount of glucose (or cellulose) and NaOH solution were first loaded into the reactor as the first step. After a given time, the reactor was immersed in a cold-water bath to terminate the reaction and to complete the first step. Then, a certain amount of $NaHCO_3$ in solid powder form was added into the reactor and it was sealed and heated. After a given time, the reactor was cooled down to room temperature to complete the second step of the reaction. In all experiments, gaseous and liquid samples were collected and analyzed (details in Supplementary Materials).

Operando hydrothermal diffuse reflectance infrared Fourier transform spectroscopy (OH-DRIFTS)

Time-resolved operando hydrothermal diffuse reflectance infrared Fourier transform spectroscopy (OH-DRIFTS) was used to monitor hydrothermal reactions. The OH-DRIFTS system was composed of an infrared (IR) spectrometer (Thermo Fisher, iS10), an observation enclosure, a high-pressure / high-temperature reaction cell with diamond windows useable at 250 °C for pressures up to 30 MPa, a heating system, a high-pressure pump and a cooling system. Schematic drawings of the equipment are shown in Fig. S2.

When monitoring hydrothermal reactions, desired amounts of reactants and water were sealed in the reaction cell, which was then put into the observation enclosure. After reaching the desired reaction temperature, OH-DRIFTS spectra were collected as the reaction progressed. When monitoring the $NaHCO_3$ reduction with glycolaldehyde, the spectrum of glycolaldehyde or $NaHCO_3$ solution alone were subtracted as background. Using the OH-DRIFTS database, the spectrum of water was subtracted as background from all spectra.

The reason for using glycolaldehyde (C2 aldose) instead of glucose for studying reduction reactions with $NaHCO_3$ in the OH-DRIFTS system is that small aldoses are intermediates of glucose and the reaction mechanism with glucose or small aldoses (including glycolaldehyde) is the same since the reduction is fulfilled by an aldehyde group. More importantly, glycolaldehyde has a simple chemical structure which avoids glucose side reactions such as dehydration, isomerization or degradation.

Evaluation of reduction efficiency

The efficiency of CO_2/$NaHCO_3$ reduction with carbohydrates was determined by the proportion of CO_2/$NaHCO_3$ generated formate to concentration of carbohydrates added to the system. The equation used for evaluation of efficiency of CO_2/$NaHCO_3$ reduction with carbohydrates (glucose or cellulose) can be written as follows:

$$\text{Formate yield}(\%) = \frac{\text{CO}_2/\text{NaHCO}_3\text{generated formate(mol/L)}}{\text{Concentration of carbohydrate(mol/L)}} \times 100\% \quad (1)$$

Details for determining CO_2/$NaHCO_3$ generated formate can be found in Supplementary Materials.

Results and discussion

CO_2/$NaHCO_3$ reduction with glucose

Reduction of CO_2 was first studied with glucose as a model compound for carbohydrates using stainless-steel tube reactors at conditions of (200 − 300) °C and (10 − 20) MPa to mimic natural submarine hydrothermal vents (T ≤ 400 °C and p ≤ 100 MPa). [19–21] However, negligible formic acid was obtained despite varying reaction settings of temperature, time and water filling. Encouragingly, formation of formate was clearly observed when alkali was introduced into the system (Table S1), i.e., when gaseous CO_2 was sealed with 1 mol/L NaOH solution for saturation before the reaction. Further experiments of varying solution pH showed a maximum in formate formation with optimal formate production being observed for pH values of around 9 (Fig. S3).

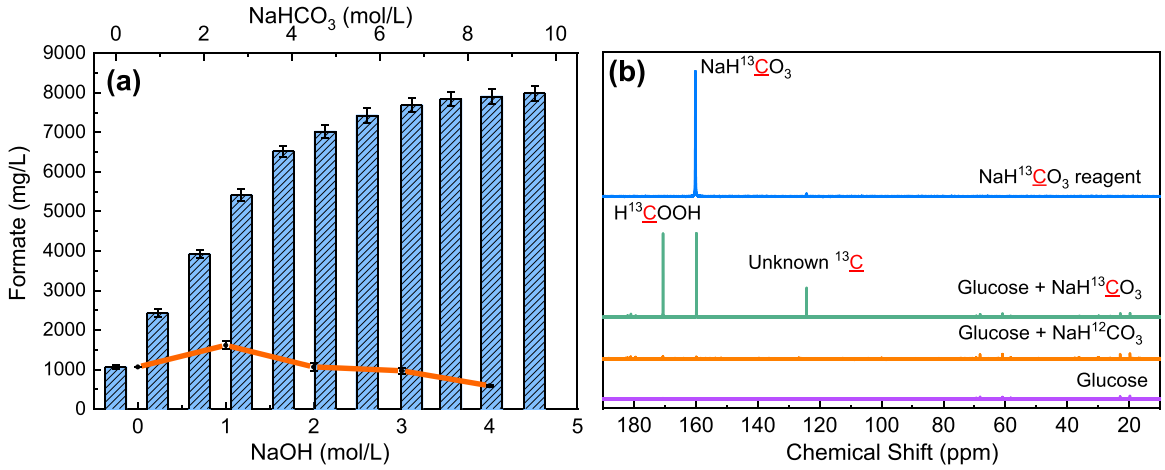

Fig. 1. $NaHCO_3$ reduction with glucose in hot water. (a) Formate production from glucose reaction with NaOH (orange line, bottom axis) or $NaHCO_3$ (solid bars, upper axis) (0.24 mol/L glucose, 1 h, 300 °C). (b) ^{13}C NMR spectra of glucose reaction with $NaH^{12}CO_3$ or $NaH^{13}CO_3$ (0.24 mol/L glucose, 6 mol/L $NaH^{12}CO_3$ or $NaH^{13}CO_3$, 300 °C, 1 h).

Since HCO_3^- is the dominant carbon species in this pH region (Fig. S4), it can be suggested that it is necessary to convert gaseous CO_2 into HCO_3^- species before formate is able to form.

Since formate can be also produced from glucose under hydrothermal alkaline conditions, [45] further experiments were performed to investigate the contribution of CO_2 reduction to formate production. $NaHCO_3$ was used to replace CO_2 because the key to formate production was in transforming CO_2 into HCO_3^- as aforementioned. Furthermore, in abiotic reduction of dissolved CO_2 in natural submarine alkaline hydrothermal systems, HCO_3^- is the dominant anion in dissolved carbon species. [17,46,47] As an experimental control on the method, experiments with glucose were conducted in the absence as well as in the presence of $NaHCO_3$. The experiments involved: (i) examination of formate production by varying pH to confirm that increased formate formation in the presence of $NaHCO_3$ was not due to changes in pH; (ii) examination of H_2 production; (iii) evaluation of the effect of reaction conditions on formate production. In experiment 1, the highest formate concentration (1600 ppm) with glucose was much lower than that (7423 ppm) with $NaHCO_3$ (Fig. 1a) indicating the contribution of $NaHCO_3$ reduction to formate formation. In experiment 2, H_2 gas formation increased with increasing NaOH concentration in the case of only glucose, whereas H_2 gas formation greatly decreased with increasing $NaHCO_3$ (Fig. S5) which suggested that the hydrogen in glucose was consumed by $NaHCO_3$ reduction to formate. However, this does not indicate that gaseous H_2 is the reductant for $NaHCO_3$ as a decrease of H_2 is caused by hydrogen consumption prior to the formation of molecular H_2 as shown later in the mechanistic study. Finally, experiment 3 showed that with coexisting $NaHCO_3$ and glucose, reaction conditions had a large effect on formate yield, whereas with only glucose, no significant changes in formate production were observed (Fig. S6). These results provide strong evidence that the increase in formate concentration in the coexisting system of $NaHCO_3$ and glucose under hydrothermal conditions was due to the reduction of $NaHCO_3$.

Direct evidence for $NaHCO_3$ reduction to formate was obtained by distinguishing formate from different sources with ^{13}C NMR measurements based on following line of thought: if a signal of ^{13}C in formate appears in ^{13}C NMR when $NaH^{13}CO_3$ is used, the observed signal should directly infer $NaHCO_3$ reduction to formate. As shown in Fig. 1b, for reaction with $NaH^{12}CO_3$ and glucose, no NMR signal of $H^{13}COO^-$ was observed. In contrast, in a labeled experiment using $NaH^{13}CO_3$, a strong signal associated with $H^{13}COO^-$ was detected at 168.2 ppm, which clearly confirmed $NaHCO_3$ reduction to formate with glucose as the reductant. Furthermore, an enhanced signal of CH_3COOH was observed in ^{13}C NMR, suggesting that $NaHCO_3$ reduction to acetic acid was also achieved in the system (enlarged spectra of glucose reaction with $NaH^{13}CO_3$ in Fig. S7). Quantification of $NaHCO_3$ reduction was made by examining formate production from $NaHCO_3$ with ^{13}C-QNMR. $CH_3{}^{13}COOH$ was deliberately selected as internal standard because the -COOH group in formic acid and acetic acid have identical sensitivities in NMR analysis (detailed quantification method in Supplementary Materials). Formate yield from $NaHCO_3$ was approximately 34% under optimized conditions, indicating that the hydrothermal CO_2 reduction with carbohydrate is highly efficient.

Hydrogen source for CO_2/$NaHCO_3$ reduction and mechanism

Possible hydrogen sources for CO_2/$NaHCO_3$ reduction include (i) H_2 generated from the carbohydrate reforming in water and (ii) direct hydrogen transfer from the carbohydrate to CO_2/$NaHCO_3$. To study how the reductive hydrogen in the carbohydrate became associated and reduced CO_2/$NaHCO_3$, time-dependent variation of intermediates and products were observed for glucose reducing $NaHCO_3$. As shown in Fig. S8a, $NaHCO_3$ reduction began after 10 min and formate increased continuously thereafter. Glucose generated small aldoses with carbon numbers from 2 to 5, which were gradually consumed as $NaHCO_3$ was reduced and aldonic acids such as glycolic acid, the oxidized product of C2 aldose, were observed (Fig. S8b). Finally, formic acid and acetic acid were produced as oxidation products of glucose. Thus, glucose generated small aldoses for $NaHCO_3$ reduction due to its aldehyde group that was then converted to the carboxyl group, leading to the formation aldonic acids as intermediates and carboxylic acids as products (other products from glucose conversion are listed in Table S2).

From these results, it can be tentatively proposed that CO_2/$NaHCO_3$ was reduced through carbohydrate hydrogen transfer, since the aqueous reforming of carbohydrates commonly generates alkanes apart from H_2 as products; [24] possible reaction pathways are shown in Fig. 2. The nucleophilic aldehyde group is what reduces the HCO_3^- into $HCOO^-$ as glucose is oxidized to gluconic acid, most likely through direct hydrogen transfer from the aldehyde group to $NaHCO_3$. Then, gluconic acid undergoes direct α-scission to form formic acid and pentose (C5 aldose). Subsequently, a similar reaction to the HCO_3^- reduction with the aldehyde group in glucose proceeds stepwise to reduce the carbon number of pentose with production of formate. As a result, a total of twelve formate/formic acid molecules are produced from the reduction of $NaHCO_3$ by glucose, with half of them being derived from $NaHCO_3$ and the other half being derived from glucose (pathway I). On the other hand, a significant increase of acetic acid was observed as product, thus pathway II – involving first dehydration then decarboxylation as side reactions – appears likely to occur in the reaction (Fig. 2, Pathway II). In total, by pathway II, glucose reduces two $NaHCO_3$

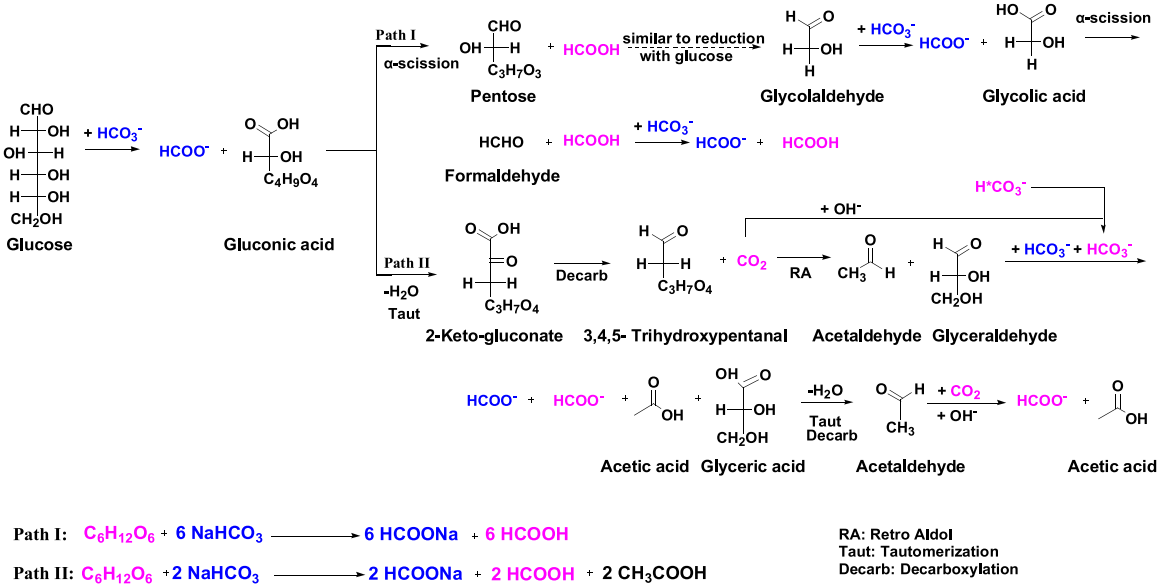

Fig. 2. Proposed reaction pathways of $NaHCO_3$ reduction with glucose (reactant $NaHCO_3$/its reduced $HCOO^-$ and glucose formed $NaHCO_3$/its reduced HCOOH are depicted in blue and violet, respectively).

molecules with itself oxidized into two formic acid and two acetic acid molecules. Notably, Pathway I surpasses Pathway II, in that Pathway I reduces four more $NaHCO_3$ molecules than Pathway II.

Direct hydrogen transfer mechanism

Further support for direct hydrogen transfer from the aldehyde group to $NaHCO_3$ type of mechanism – the key step in $NaHCO_3$ reduction – was provided by OH-DRIFTS measurements for which $NaHCO_3$ reduction with glycolaldehyde (C2 aldose) was used instead of glucose to eliminate by-product noise (details in Supplementary Materials). As this was the first time that OH-DRIFTS had been used to observe hydrothermal reduction of CO_2/$NaHCO_3$ with carbohydrates, an OH-DRIFTS database of reactants and possible intermediates was built beforehand (Fig. S9). The OH-DRIFTS spectra of $NaHCO_3$ reduction with glycolaldehyde are shown in Fig. 3 in which signals at ca. 1279 cm^{-1} and 1395 cm^{-1} can be assigned to formaldehyde and glycolic acid, [48] respectively. As shown in Fig. 3, signals for formaldehyde and glycolic acid gradually intensified and later flattened, representing intermediates, further supporting the proposed reaction pathways shown in Fig. 2, namely, that aldose was first oxidized to aldonic acid and later degraded to smaller aldoses with one less carbon to achieve $NaHCO_3$ reduction.

Signals in the region of (2800–3000) cm^{-1} were assigned to ν(C-H) mode of formate in light of the built OH-DRIFTS database (Fig. S9). Besides continuous growth, peaks of ν(C-H) became blue-shifted after 15 min (Fig. 4a and b), which represents an elevated C-H bond energy. Based on the inductive effect, this enhanced C-H bond energy is likely to be caused by another functional group linked to the C atom, as it dispersed the electron cloud of center C. Hence, this shift could suggest the formation of orthoformate ($HCO(OH)_2^-$), the hydrated formate, which transforms to formate through loss of H_2O (Fig. 4d). Although the existence of orthoformate has been supported by ab initio computations, [49,50] it is quite difficult to isolate orthoformate due to its activity. Thus, further support for this shift to orthoformate was acquired by FTIR signals of esterified compounds of formic acid and orthoformic acid, $HCO(OCH_3)$ and $HC(OCH_3)_3$. The wavenumber of ν(C-H) in $HC(OCH_3)_3$ was also higher than that of $HCO(OCH_3)$ (Fig. S10a), demonstrating that the shift of ν(C-H) in formate was probably due to the formation of orthoformate. When gaseous H_2 is used in $NaHCO_3$ reduction, $NaHCO_3$ is reduced to formate directly as it is thermodynamically favored. [51,52] However, no similar shift of ν(C-H) in formate was observed in OH-DRIFTS spectra of $NaHCO_3$ reduction with gaseous H_2 (Fig. S11). Thus, the detection of orthoformate here demonstrated that rather than being reduced by gaseous H_2 from glucose oxidation, the $NaHCO_3$ was reduced via hydrogen transfer between glucose (aldehyde group) and $NaHCO_3$. Indeed, when ex-situ H_2 (1 MPa) was applied as reductant, only a small amount of formate (less than 200 mg/L) was produced, further confirming the advocated hydrogen transfer mechanism, and more importantly suggesting its crucial contribution to the high reduction efficiency of $NaHCO_3$.

Catalytic role of hot water in direct hydrogen transfer

With confirmation of the hydrogen source for $NaHCO_3$ reduction being determined, we were curious in how hydrogen transfer could proceed so efficiently between $NaHCO_3$ and the carbohydrate even without the addition of a heterogeneous catalyst. To address this point, OH-DRIFTS spectra of $NaHCO_3$ reduction with glycolaldehyde were further analyzed, focusing on signals in the region of (1000–1200) cm^{-1}, the typical stretching mode of C-O bond (ν(C-O)). Enlarged spectra revealed that three peaks at ca. (1032, 1082, 1125) cm^{-1} evolved with reaction progress and flattened as the reaction approached completion (Fig. 4c), indicating that the peaks were reaction intermediates. These signals were further ascribed to the C-O bond of hydrated formaldehyde and glycolaldehyde by analyzing the self-built OH-DRIFTS database when considering inductive effects (Figs. S9b and S9c) and excluding the formation of methanol and ethylene glycol from formaldehyde and glycolaldehyde by Cannizzaro reaction (Fig. S10b, analysis details in Supplementary Materials). Thus, peaks at ca. 1082 cm^{-1} and 1125 cm^{-1} were assigned to hydrated glycolaldehyde, and the peak at ca. 1032 cm^{-1} was assigned to hydrated formaldehyde.

When a -CHO group becomes hydrated, reductive hydrogen attached to the center carbon of a molecule becomes nucleophilic, which can easily reduce electron deficient substances. [53] Thus, when molecular water hydrates the -CHO group to form $-CH(OH)_2$, reductive hydrogen becomes so active that it can directly attack $NaHCO_3$ molecules through hydrogen transfer. The mechanism is detailed in Fig. 4d taking glycolaldehyde as the representative carbohydrate. When the -CHO group in glycolaldehyde is hydrated, a six-member ring transition state results with HCO_3^-, leading to the formation of a C-H bond between highly activated hydrogen and HCO_3^- through nucleophilic

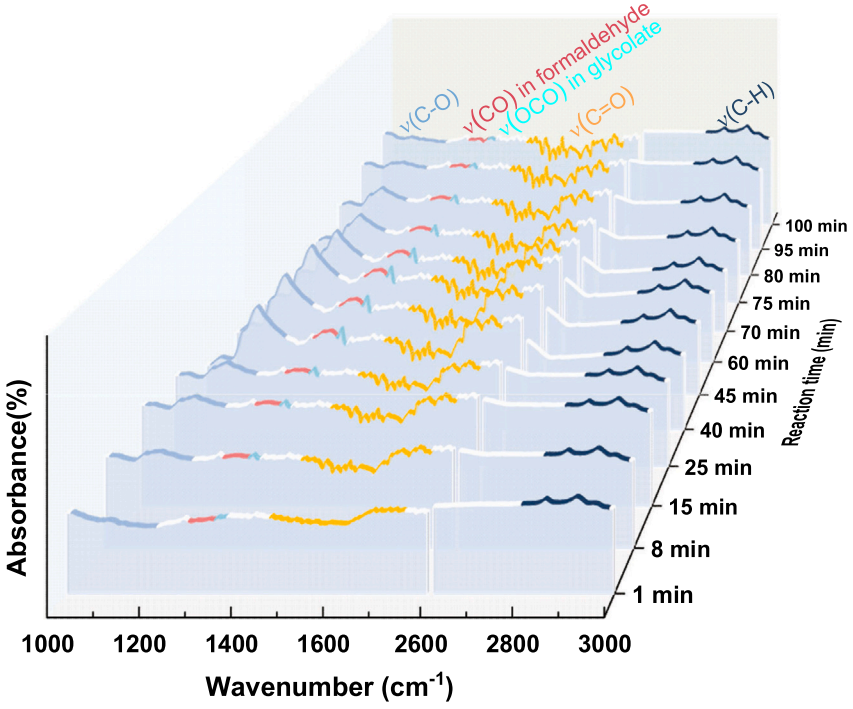

Fig. 3. OH-DRIFTS spectra of $NaHCO_3$ reduction with glycolaldehyde in hot water (0.9 mol/L $NaHCO_3$, 0.125 mol/L glycolaldehyde, 250 °C, autogenous pressure).

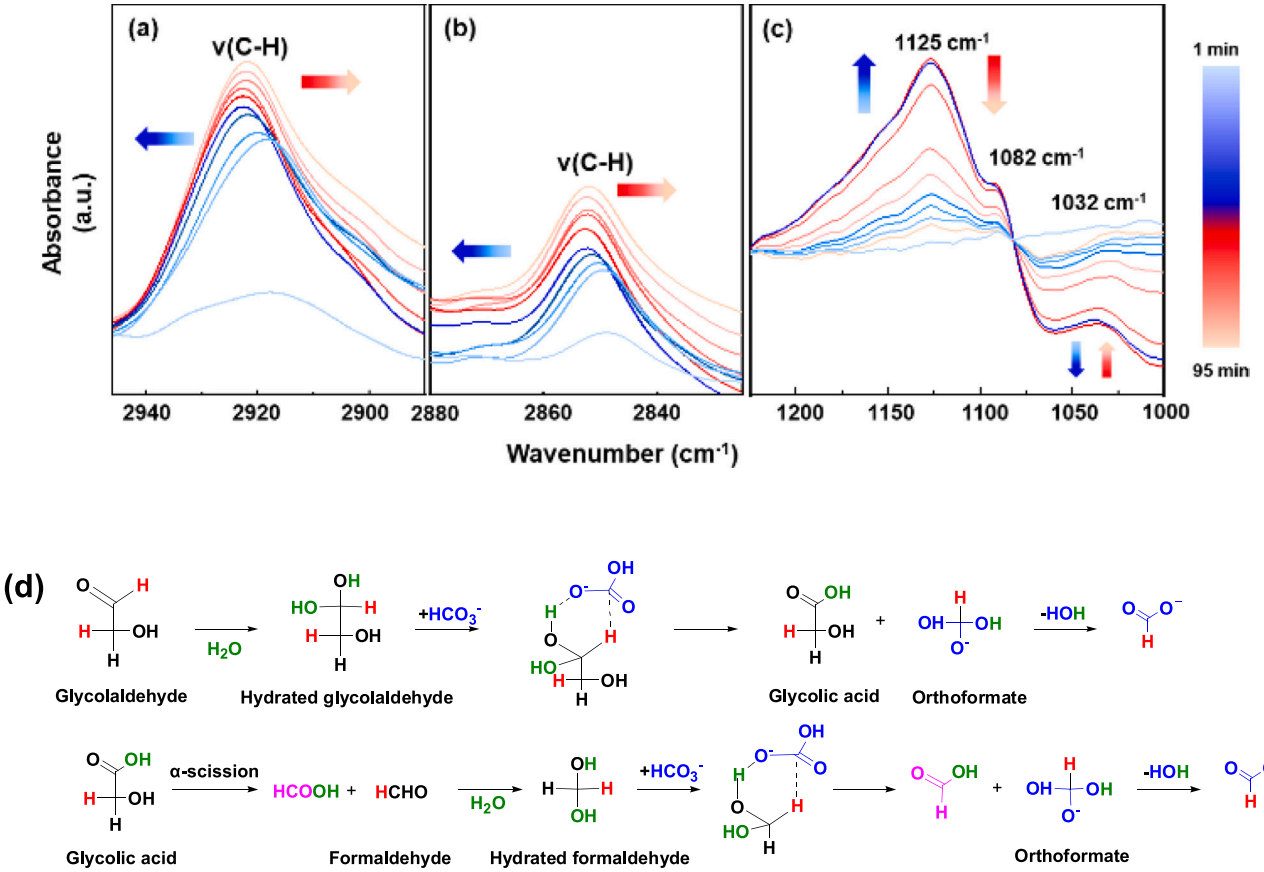

Fig. 4. Enlarged OH-DRIFTS spectra of $NaHCO_3$ reduction with glycolaldehyde and showing catalytic role of water in hydrogen transfer. (a and b) Enlarged signal of ν(C-H) in formate. (c) Enlarged signal of ν(C-O) in hydrated glycolaldehyde and formaldehyde. (d) Catalytic role of water in hydrogen transfer for $NaHCO_3$ reduction (reactant $NaHCO_3$/its reduced $HCOO^-$ and glycolaldehyde formed HCOOH are depicted in blue and violet, respectively. Reductive hydrogen in glycolaldehyde is exhibited in red, and H_2O catalyzing the reaction is shown in green).

addition of a C═O bond. Thereafter, HCO_3^- is reduced to orthoformate and glycolaldehyde is oxidized to glycolic acid. Subsequently, orthoformate loses H_2O to form formate, while glycolic acid undergoes direct α-scission to formic acid and formaldehyde, which then reduces $NaHCO_3$ by repeating the above steps until completion. It is known that water under hydrothermal conditions has unique properties such as high H^+/OH^- concentrations that promote acid/base catalyzed reactions. [54] However, the role of molecular water as a homogeneous catalyst has scarcely been probed with few such examples being elucidated based on DFT calculations. [55] Here, with OH-DRIFTS, it could be experimentally verified that water catalyzes $NaHCO_3$ reduction by converting the -CHO group in a carbohydrate to its hydrated state as $-CH(OH)_2$, which enabled $NaHCO_3$ reduction through hydrogen transfer, thus obviating the need for noble metal-based catalysts.

Hot water as hydrogen source for $NaHCO_3$ reduction

After determining how hydrogen in a carbohydrate became associated and then reduced $NaHCO_3$, it was necessary to consider if water could act as a hydrogen source in the reduction of $NaHCO_3$. If so, with solar energy naturally stored in biomass, biomass invoked water splitting for CO_2 reduction could possibly lead to an altered mode of artificial photosynthesis. Generally, experiments with D_2O are employed for checking the reactive behavior of water; however, considering H-D exchange of glucose in D_2O due to its isomerization to ketose, [56] reactions were conducted with glycolaldehyde reducing $NaHCO_3$ in D_2O. As expected, no H-D exchange was observed when only glycolaldehyde reacted under hydrothermal conditions (Fig. S12). Intriguingly, during $NaHCO_3$ reduction with glycolaldehyde in D_2O, $DCOO^-$ was formed (Fig. 5a), which is a clear demonstration that water is one of the hydrogen sources in $NaHCO_3$ reduction and that carbohydrates are an energy source capable of splitting water for CO_2 reduction. The contribution of water to the reduction of $NaHCO_3$ was further assessed by quantifying the $DCOO^-$ content of total formate with ^{2}H-QNMR measurements. $DCOO^-$ accounted for 12.3% of total formate, i.e., the ratio of hydrogen from water and glycolaldehyde for $NaHCO_3$ reduction was about 13:87 on an atom basis. From previous discussion, the mechanism by which water is hypothesized to act as a hydrogen source is depicted in Fig. 5b: the -CHO group becomes hydrated to attack surrounding water molecules in a similar process to how $-CH(OH)_2$ reduces $NaHCO_3$ through hydrogen transfer, thus generating a highly active H···H intermediate leading to $NaHCO_3$ reduction.

Enhancement of CO_2 reduction and assessment of reaction energy budget

Based on the proposed reaction pathways in Fig. 2, if glycolaldehyde could be selectively produced from glucose, enhanced $NaHCO_3$ reduction might be obtained since side reactions such as dehydration and tautomerization would be avoided. Thus, a two-step reaction strategy was formulated to enhance CO_2 reduction in which the first-step reaction was designed to accelerate the formation of intermediates such as glycolaldehyde from glucose at low-temperatures (ca. 25 °C), or via short reaction times at high-temperatures (ca. 300 °C). For the first-step reaction, formate yield increased to about 44% in 7 h at 25 °C (Fig. 6), and more encouragingly, a maximum formate yield of 55% was achieved in 40 s at 300 °C (Fig. 6). Thus, a formate productivity of 0.069 mol/L h^{-1} could be attained in the reaction, which was relatively a promising result comparing to other reported values through catalytic hydrogenation or photo-catalytic reactions (as listed in Table S3).

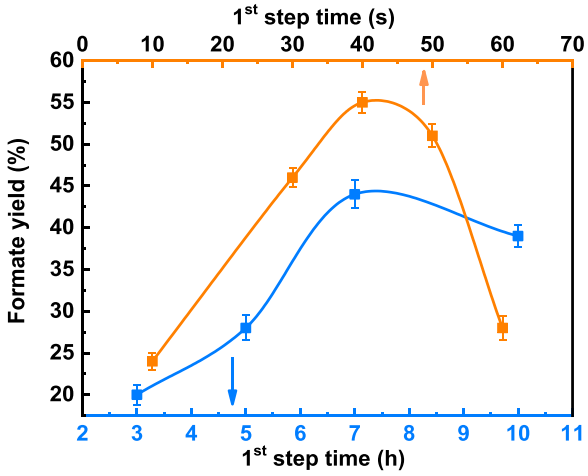

Fig. 6. Variation of formate yields in water with first-step reaction time (0.125 mol/L glycolaldehyde, 3 mol/L $NaHCO_3$, first-step reaction was performed at 25 °C (blue line) and 300 °C (orange line), respectively, and second step reaction was performed at 300 °C for 1 h).

Next, $NaHCO_3$ reduction with cellulose was considered. The ^{13}C NMR analysis for $NaH^{13}CO_3$ reaction with cellulose showed a strong $H^{13}COO^-$ signal (Fig. 7a), clearly confirming $NaHCO_3$ reduction into formate with cellulose. $NaHCO_3$ reduction through direct use of a biopolymer provides key experimental evidence that hydrothermal reduction of CO_2 with biomass occurs. By optimizing the two-step reaction strategy, a maximum formate yield of 76% was achieved, with an even higher yield than that with glucose being obtained when the first-step reaction was performed at 300 °C for 120 s (Fig. 7b). The enhanced formate yield for cellulose is possibly due to glycolaldehyde being highly efficient in $NaHCO_3$ reduction. Moreover, glycolaldehyde can be selectively produced from slow hydrolysis of cellulose, restricting the production of other small aldoses (such as C3 and C4 aldose) than in the case with glucose. In fact, only very minor formation of acetic acid and the smallest trace of lactic acid were detected with cellulose as

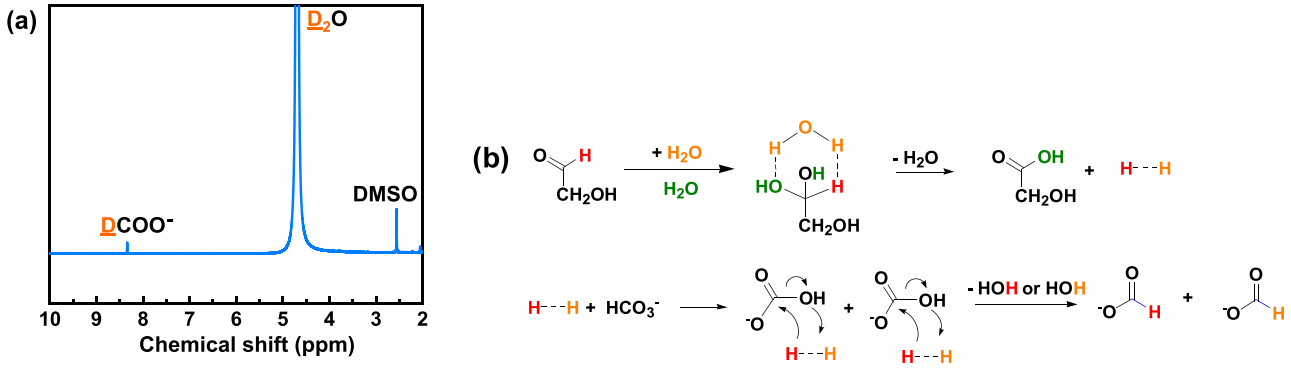

Fig. 5. Role of water as hydrogen source for NaHCO3 reduction. (a) 2H NMR spectrum of $NaHCO_3$ reduction with glycolaldehyde in D_2O (0.125 mol/L glycolaldehyde, 3 mol/L $NaHCO_3$, 1 h, 300 °C). (b) Mechanism of water as hydrogen source (taking glycolaldehyde as the representative of carbohydrate – the hydrogen source in water and glycolaldehyde is shown in yellow and red respectively while the H_2O catalyzing reaction is shown in green).

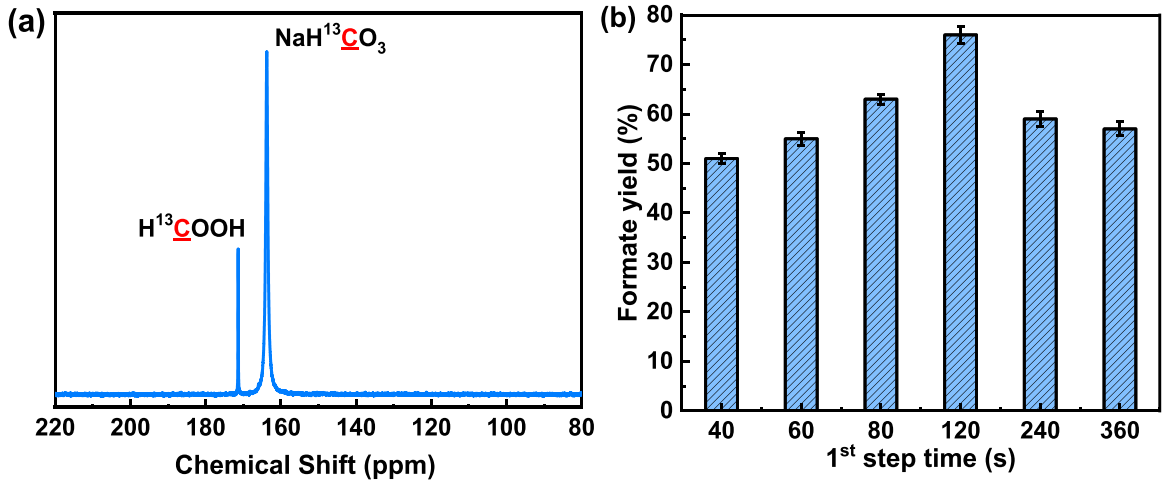

Fig. 7. $NaHCO_3$ reduction with cellulose in hot water. (a) ^{13}C NMR spectrum of $NaH^{13}CO_3$ reaction with cellulose (0.125 mol/L cellulose, 3 mol/L $NaH^{13}CO_3$, 300 °C, 1 h). (b) Variation of formate yields with first-step reaction time (0.125 mol/L cellulose, 3 mol/L $NaHCO_3$, first-step reaction was performed at 300 °C, and second step reaction was performed at 300 °C for 1 h).

reductant which are products that easily obtained from C3 or C4 aldose oxidation (Fig. S13).

To see whether or not a net carbon benefit could be realized with carbohydrate-enabled CO_2 reduction, product distributions were analyzed, where it was found that H_2 was the only gaseous product and glucose was converted to formic acid and acetic acid (Fig. S5). Thus, CO_2 was solely assimilated in the reduction.

Thermodynamic data of CO_2 reduction with carbohydrates was determined based on the proposed reaction pathways (Fig. 2). Calculated reaction enthalpy and Gibbs energy were both negative (Eqs. (2) and (3)), indicating $NaHCO_3$ reduction with glucose was not only spontaneous, but also exothermic, that is, glucose provides an energy source for $NaHCO_3$ reduction, thereby saving expense of other kinds of energy consumption to afford a net carbon benefit.

$$C_6O_6H_{12}\ (s) + 6HCO_3^-\ (aq) \rightarrow 6HCOO^-\ (aq) + 6HCOOH\ (aq)$$

$$\Delta rH = -854{\cdot}46\ kJ/mol\ \Delta rG = -271{\cdot}96\ kJ/mol\ T = 573{\cdot}15\ K \quad (2)$$

$$C_6O_6H_{12}\ (s) + 2HCO_3^-\ (aq) \rightarrow 2HCOO^-\ (aq) + 2HCOOH\ (aq) + 2CH_3COOH\ (aq)$$

$$\Delta rH = -890{\cdot}74\ kJ/mol\ \Delta rG = -327{\cdot}53\ kJ/mol\ T = 573{\cdot}15\ K \quad (3)$$

The production of formic acid and acetic acid from glucose demonstrates that in the proposed system, both $NaHCO_3$ and glucose are converted into valuable chemicals indicating high atomic efficiency. As worldwide demand for formic acid continues to grow, especially as a renewable hydrogen carrier, [57–59] formic acid production from both CO_2 and carbohydrates in one reaction system can be more sustainable than existing routes.

As carbohydrates provide an energy source for CO_2 reduction, and with the consideration of energy consumption of hydrothermal reactions, fundamental assessment of energy efficiency of solar (contained in carbohydrate) to fuel (formate) was performed. First, total energy input (Q_{input}) and output (Q_{output}) of the reactions were determined. CO_2 reduction with carbohydrates under hydrothermal conditions comprises three steps: heating (HT) and cooling (CL) of the reaction solution, and the reaction (RE) itself. As shown in Fig. 8, during HT, thermal processes can be divided into four parts. In RE, a certain amount of reaction heat can be collected, which is the enthalpy change of reaction in Eq. (2) with consideration of heat loss based on Carnot's theorem (Q_{RE}). During CL, the reaction solution is cooled down to ambient temperature so that solution heat can be also collected with consideration of heat loss also based on Carnot's theorem (Q_{CL}).

Thus, if one mole of reactant (glucose) is considered, total energy input (Q_{input}) of the reaction is determined as 7272.12 kJ by the following equation (calculations in Supplementary Materials):

$$Q_{input} = 1 \times \Delta rG^o_{glucose} + Q_{HT} - Q_{RE} - Q_{CL} \quad (4)$$

Total energy output (Q_{output}) is $12 \times \Delta rG^o_{HCOOH}$ based on Eq. (2), and ΔrG^o_{HCOOH} is determined regarding energy density of HCOOH as 240.27 kJ/mol. [60] Thus, $Q_{output} = 12 * 240.27 = 2883.24$ kJ/mol.

Then, the theoretical solar-to-formate energy efficiency ($\eta_{solar\text{-}to\text{-}formate}$) via CO_2 reduction with carbohydrates was determined assuming the use of the solar energy "trapped" in the carbohydrate and coupling

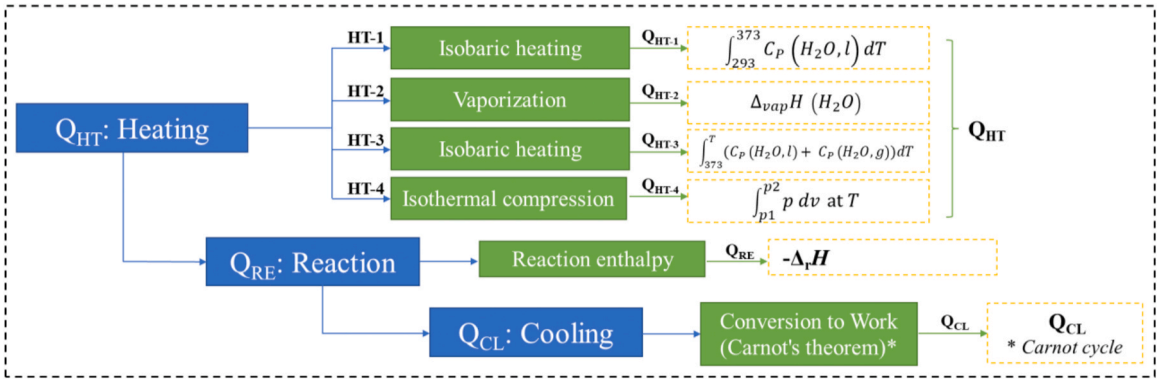

Fig. 8. System boundary of CO_2 reduction with carbohydrates in hot water.

with photovoltaic devices. In terms of energy input, photosynthesis efficiency of plants (η_{PE}) is considered for $\Delta rG^{o}_{glucose}$, and for "Q_{HT} - Q_{RE} - Q_{CL}", with solar energy being first transferred into electricity (η_{SEE}) and then electricity being used to heat the reaction system (η_{EHR}). Thus, theoretical solar-to-formate energy efficiency ($\eta_{solar\text{-}to\text{-}formate}$) can be expressed as:

$$\eta_{solar-to-formate} = \frac{12 \times \Delta rG^{o}\, HCOOH}{\frac{1 \times \Delta rG^{o}\, glucose}{\eta_{PE}} + \frac{HT(Q) - RE(Q) - CL(Q)}{\eta_{SEE} \times \eta_{EHR}}} \quad (5)$$

According to general information available for η_{PE}, η_{SEE} and η_{EHR}, theoretical solar-to-formate efficiency was determined to be 3.4% (calculations in Supplementary Materials). When further considering the optimal reaction efficiency of CO_2 reduction of 76% here, attainable solar-to-formate efficiency is 2.6% (3.4% * 76% = 2.6%), which is over twice that reported for optimal solar-to-formate energy conversion efficiencies of artificial photosynthesis (approximately 1%). [4] More encouragingly, if gene regulated plants are used as reactants, that is 8% photosynthesis efficiency for plants, [61,62] it follows that a solar-to-formate energy efficiency of 3.4% could be attained.

Conclusions

This work describes a geochemically-inspired strategy for efficient CO_2 reduction with carbohydrates in hot water. The study shows that reduction of CO_2/$NaHCO_3$ into formate by cellulose occurs in yields as high as 76%, and carbohydrates are oxidized to value-added carboxylic acids. Thus, carbohydrate-enabled CO_2 reduction based on $NaHCO_3$ conversion to formate has potential application with net carbon zero emission benefits. OH-DRIFTS spectra revealed that hot water acts as a homogeneous catalyst in $NaHCO_3$ reduction by hydrating the -CHO group in a carbohydrate into -$CH(OH)_2$. These findings provide basic reaction chemistry on CO_2 reduction with carbohydrates in hot water by employing in situ spectroscopic techniques that support the development of future biomass-enabled CO_2 reduction processes. The results in this study broaden the knowledge database of molecular interactions between carbohydrates and inorganic compounds in hydrothermal environments and expand the applications of hydrothermal chemistry for developing net carbon zero emission processes.

CRediT authorship contribution statement

Conceptualization: **YY**, **FMJ**, **YHY**; Methodology: **YY**, **HZ**, **JC**; Investigation: **YY**, **HZ**, **JC**; Visualization: **YY**, **JC**; Supervision: **FMJ**; Writing – original draft: **YY**; Writing – review & editing: **YY**, **FMJ**, **YHY**, **RLS Jr**.

Declaration of Competing Interest

The authors declare that they have no known competing financial interests or personal relationships that could have appeared to influence the work reported in this paper.

Acknowledgments

The authors thank the financial support of the National Natural Science Foundation of China (No. 21978170 & 22108171), the Natural Science Foundation of Shanghai (No. 23ZR1435200), and Shanghai Key Laboratory of Hydrogen Science & Center of Hydrogen Science, Shanghai Jiao Tong University, China.

Appendix A. Supporting information

Supplementary data associated with this article can be found in the online version at doi:10.1016/j.nxener.2023.100037.

References

[1] L. Ji, L. Li, X. Ji, Y. Zhang, S. Mou, T. Wu, Q. Liu, B. Li, X. Zhu, Y. Luo, X. Shi, A. Asiri, X. Sun, Highly selective electrochemical reduction of CO_2 to Alcohols on an FeP Nanoarray, Angew. Chem. Int. Ed. 59 (2020) 758–762, https://doi.org/10.1002/ange.201912836

[2] S. Mou, T. Wu, J. Xie, Y. Zhang, L. Ji, H. Huang, T. Wang, Y. Luo, X. Xiong, B. Tang, X. Sun, Boron phosphide nanoparticles: a nonmetal catalyst for high-selectivity electrochemical reduction of CO_2 to CH_3OH, Adv. Mater. 31 (2019) 1903499, https://doi.org/10.1002/adma.201903499

[3] R. Zhao, P. Ding, P. Wei, L. Zhang, Q. Liu, Y. Luo, T. Li, S. Lu, X. Shi, S. Gao, A. Asiri, Z. Wang, X. Sun, Recent progress in electrocatalytic methanation of CO_2 at ambient conditions, Adv. Funct. Mater. 31 (2021) 2009449, https://doi.org/10.1002/adfm.202009449

[4] J.Y. Loh, N.P. Kherani, G.A. Ozin, Persistent CO_2 photocatalysis for solar fuels in the dark, Nat. Sustain. 4 (2021) 466–473, https://doi.org/10.1038/s41893-021-00681-y

[5] J. Zhou, J. Li, L. Kan, L. Zhang, Q. Huang, Y. Yan, Y. Chen, J. Liu, S. Li, Y. Lan, Linking oxidative and reductive clusters to prepare crystalline porous catalysts for photocatalytic CO_2 reduction with H_2O, Nat. Commun. 13 (2022) 4681, https://doi.org/10.1038/s41467-022-32449-z

[6] U. Kang, S.K. Choi, D.J. Ham, S.M. Ji, W. Choi, D.S. Han, A. Abdel-Wahab, H. Park, Photosynthesis of formate from CO_2 and water at 1% energy efficiency via copper iron oxide catalysis, Energy Environ. Sci. 8 (2015) 2638–2643, https://doi.org/10.1039/c5ee01410g

[7] T. Arai, S. Sato, T. Kajino, T. Morikawa, Solar CO_2 reduction using H_2O by a semiconductor/metal-complex hybrid photocatalyst: enhanced efficiency and demonstration of a wireless system using $SrTiO_3$ photoanodes, Energy Environ. Sci. 6 (2013) 1274–1282, https://doi.org/10.1039/c3ee24317f

[8] W. Wang, S.P. Wang, X.B. Ma, J.L. Gong, Recent advances in catalytic hydrogenation of carbon dioxide, Chem. Soc. Rev. 40 (2011) 3703–3727, https://doi.org/10.1039/c1cs15008a

[9] S. Navarro-Jaén, M. Virginie, J. Bonin, M. Robert, R. Wojcieszak, A.Y. Khodakov, Highlights and challenges in the selective reduction of carbon dioxide to methanol, Nat. Rev. Chem. 5 (2021) 564–579, https://doi.org/10.1038/s41570-021-00289-y

[10] S. Choi, T.C. Davenport, S.M. Haile, Protonic ceramic electrochemical cells for hydrogen production and electricity generation: exceptional reversibility stability and demonstrated faradaic efficiency, Energy Environ. Sci. 12 (2019) 206–215, https://doi.org/10.1039/c8ee02865f

[11] R.M. Navarro, M.A. Peña, J.L.G. Fierro, Hydrogen production reactions from carbon feedstocks: fossils fuels and biomass, Chem. Rev. 107 (2007) 3952–3991, https://doi.org/10.1021/cr0501994

[12] F. Sha, X. Liu, S. Tang, J. Wang, C. Li, Hydrogenation of CO_2 to Chemicals with Green Hydrogen, Vol. 2, Ch. 25, in: K. Ding, X.-F. Wu, B. Han, Z. Liu (Eds.), The chemical transformations of C1 compounds, WILEY-VCH GmbH, 2022, pp. 1073–1184 Vol. 2, Ch. 25.

[13] F.M. Jin, Y. Gao, Y.J. Jin, Y.L. Zhang, J.L. Cao, Z. Wei, R.L. Smith Jr., High-yield reduction of carbon dioxide into formic acid by zero-valent metal/metal oxide redox cycles, Energy Environ. Sci. 4 (2011) 881–884, https://doi.org/10.1021/cr0501994

[14] D.P. He, X.G. Wang, Y. Yang, R.T. He, H. Zhong, Y. Wang, B.X. Han, F.M. Jin, Hydrothermal synthesis of long-chain hydrocarbons up to C24 with $NaHCO_3$-assisted stabilizing cobalt, e2115059118, PNAS 118 (No. 51) (2021), https://doi.org/10.1073/pnas.2115059118

[15] M.J. Russell, A.J. Hall, W. Martin, Serpentinization as a source of energy at the origin of life, Geobiology 8 (2010) 355–371, https://doi.org/10.1111/j.1472-4669.2010.00249.x

[16] M.J. Russell, W. Nitschke, E. Branscomb, The inevitable journey to being, Philos. Trans. R. Soc. Lond. B Biol. Sci. 368 (2013) 20120254, https://doi.org/10.1098/rstb.2012.0254

[17] M.J. Russell, A.J. Hall, The emergence of life from iron monosulphide bubbles at a submarine hydrothermal redox and pH front, J. Geo. Soc. 8 (1997) 96–116, https://doi.org/10.1144/gsjgs.154.3.0377

[18] J.R. Michalski, T.C. Onstott, S.J. Mojzsis, J. Mustard, Q.H.S. Chan, P.B. Niles, S.S. Johnson, The Martian subsurface as a potential window into the origin of life, Nat. Geosci. 11 (2018) 21–26, https://doi.org/10.1038/s41561-017-0015-2

[19] M.J. Russell, R.M. Daniel, A.J. Hall, J.A. Sherringham, A hydrothermally precipitated catalytic iron sulphide membrane as a first step toward life, J. Mol. Evol. 39 (1994) 231–243, https://doi.org/10.1007/BF00160147

[20] L.M. White, T. Shibuya, S.D. Vance, L.E. Christensen, R. Bhartia, R. Kidd, A. Hoffmann, G.D. Stucky, I. Kanik, M.J. Russell, Simulating serpentinization as it could apply to the emergence of life using the JPL hydrothermal reactor, Astrobiology 20 (2020) 307–326.

[21] G. Proskurowski, M.D. Lilley, J.S. Seewald, G.L. Früh-Green, E.J. Olson, J.E. Lupton, S.P. Sylva, D.S. Kelley, Abiogenic hydro-carbon production at Lost City hydrothermal field, Science 319 (2008) 604–607, https://doi.org/10.1089/ast.2018.1949

[22] T.M. McCollom, J.S. Seewald, Abiotic synthesis of organic compounds in deep-sea hydrothermal environments, Chem. Rev. 107 (2007) 382–401, https://doi.org/10.1126/science.1151194

[23] Y. Choi, R. Mehrotra, S. Lee, T. Nguyen, I. Lee, J. Kim, H. Yang, H. Oh, H. Kim, J. Lee, Y. Kim, S. Jang, J. Jang, J. Ryu, Bias-free solar hydrogen production at 19.8 mA cm^{-2} using perovskite photocathode and lignocellulosic biomass, Nat. Commun. 13 (2022) 5709, https://doi.org/10.1038/s41467-022-33435-1

[24] R.D. Cortright, R.R. Davda, J.A. Dumesic, Hydrogen from catalytic reforming of biomass-derived hydrocarbons in liquid water, Nature 418 (2002) 964–967, https://doi.org/10.1038/nature01009

[25] L. Lin, W. Zhou, R. Gao, S. Yao, X. Zhang, W. Xu, S. Zheng, Z. Jiang, Q. Yu, Y.W. Li, C. Shi, X.D. Wen, D. Ma, Low-temperature hydrogen production from water and methanol using Pt/α-MoC catalysts, Nature 544 (2017) 80–83, https://doi.org/10.1038/nature21672
[26] Z. Wei, J. Sun, Y. Li, A.K. Datye, Y. Wang, Bimetallic catalysts for hydrogen generation, Chem. Soc. Rev. 41 (2012) 7994–8008, https://doi.org/10.1039/C2CS35201J
[27] H. Luo, J. Barrio, N. Sunny, A. Li, L. Steier, N. Shah, I. Stephens, M. Titirici, Progress and perspectives in photo- and electrochemical-oxidation of biomass for sustainable chemicals and hydrogen production, Adv. Energy Mater. 11 (2021) 2101180, https://doi.org/10.1002/aenm.202101180
[28] J. Zimmerman, P. Anastas, H. Erythropel, W. Leitner, Designing for a green chemistry future, Science 367 (2020) 397–400, https://doi.org/10.1126/science.aay3060
[29] S. Gao, S. Chen, Q. Liu, S. Zhang, G. Qi, J. Luo, X. Liu, Bifunctional BiPd alloy particles anchored on carbon matrix for reversible Zn–CO_2 battery, ACS Appl. Nano Mater. 5 (9) (2022) 12387–12394, https://doi.org/10.1021/acsanm.2c02917
[30] S. Gao, T. Wei, J. Sun, Q. Liu, D. Ma, W. Liu, S. Zhang, J. Luo, X. Liu, Atomically dispersed metal-based catalysts for Zn–CO_2 batteries, Small Struct. 3 (2022) 2200086, https://doi.org/10.1002/sstr.202200086
[31] S. Liu, L. Wang, H. Yang, S. Gao, Y. Liu, S. Zhang, Y. Chen, X. Liu, J. Luo, Nitrogen-doped carbon polyhedrons confined Fe–P nanocrystals as high-efficiency bifunctional catalysts for aqueous Zn − CO_2 batteries, Small 18 (2022) 2104965, https://doi.org/10.1002/smll.202104965
[32] W. Liu, Z. Xu, D. Zhao, X. Pan, H. Li, X. Hu, Z. Fan, W. Wang, G. Zhao, S. Jin, G. Huber, H. Yu, Efficient electrochemical production of glucaric acid and H_2 via glucose electrolysis, Nat. Commun. 11 (2020) 265, https://doi.org/10.1038/s41467-019-14157-3
[33] L. Guo, X. Zhang, L. Gan, L. Pan, C. Shi, Z. Huang, X. Zhang, J. Zou, Advances in selective electrochemical oxidation of 5-Hydroxymethylfurfural to produce high-value chemicals, Adv. Sci. 10 (2023) 2205540, https://doi.org/10.1002/advs.202205540
[34] F. Jin, H. Enomoto, Rapid and highly selective conversion of biomass into value-added products in hydrothermal conditions: chemistry of acid/base-catalysed and oxidation reactions, Energy Environ. Sci. 4 (2011) 382–397, https://doi.org/10.1039/C004268D
[35] J. Luterbacher, D. Alonsoa, Martin, J. Dumesic, Targeted chemical upgrading of lignocellulosic biomass to platform molecules, Green. Chem. 16 (2014) 4816–4838, https://doi.org/10.1039/C4GC01160K
[36] G. Zhang, F. Jin, B. Wu, J. Cao, Y. Adam, Y. Wang, Hydrothermal conversion of glycerin into lactic acid by a continuous-flow reactor, Int. J. Chem. React. Eng. 10 (2012) A55, https://doi.org/10.1515/1542-6580.3055
[37] F. Jin, G. Zhang, Y. Jin, Y. Watanabe, A. Kishita, H. Enomoto, A new process for producing calcium acetate from vegetable wastes for use as an environmentally friendly deicer, Bio. Technol. 101 (2010) 7299–7306, https://doi.org/10.1016/j.biortech.2010.04.081
[38] Y. Yang, H. Zhong, R. He, X. Wang, J. Cheng, G. Yao, F. Jin, Synergetic conversion of microalgae and CO_2 into value-added chemicals under hydrothermal conditions, Green. Chem. 21 (2019) 1247–1252, https://doi.org/10.1039/C8GC03645D
[39] W. Yan, B. Jin, J. Cheng, X. Shi, H. Zhong, F. Jin, Ru/ZrO_2 as a facile and efficient heterogeneous catalyst for the catalytic hydrogenation of bicarbonate using biodiesel-waste glycerol as a hydrogen donor, ACS Sustain. Chem. Eng. 10 (2022) 5374–5383, https://doi.org/10.1021/acssuschemeng.1c07848
[40] Y. Yang, H. Zhong, G. Yao, R. He, B. Jin, F. Jin, Hydrothermal reduction of $NaHCO_3$ into formate with hexanehexol, Catal. Today 318 (2018) 10–14, https://doi.org/10.1016/j.cattod.2017.09.005
[41] W. Lee, Y. Kim, M. Youn, S. Jeong, K. Park, Catholyte-free electrocatalytic CO_2 reduction to formate, Angew. Chem. Int. Ed. 57 (2018) 6883–6887, https://doi.org/10.1002/anie.201803501
[42] E.V. Kondratenko, G. Mul, J. Baltrusaitis, G.O. Larrazabal, J. Perez-Ramirez, Status and perspectives of CO_2 conversion into fuels and chemicals by catalytic, photocatalytic and electrocatalytic processes, Energy Environ. Sci. 6 (2013) 3112–3135, https://doi.org/10.1039/C3EE41272E
[43] W.G. Tu, Y. Zhou, Z.G. Zou, Photocatalytic conversion of CO_2 into renewable hydrocarbon fuels: state-of-the-art accomplishment, challenges, and prospects, Adv. Mater. 26 (2014) 4607–4626, https://doi.org/10.1002/adma.201400087
[44] P. Savage, Organic chemical reactions in supercritical water, Chem. Rev. 99 (1999) 603–622, https://doi.org/10.1021/cr9700989
[45] F.M. Jin, J. Yun, G.M. Li, A. Kishita, K. Tohji, H. Enomoto, Hydrothermal conversion of carbohydrate biomass into formic acid at mild temperatures, Green. Chem. 10 (2008) 612–615, https://doi.org/10.1039/B802076K
[46] C. McCammon, The paradox of mantle redox, Science 308 (2005) 807–808, https://doi.org/10.1126/science.1110532
[47] T.M. McCollom, J.S. Seewald, A reassessment of the potential for reduction of dissolved CO_2 to hydrocarbons during serpentinization of olivine, Geochim. Cosmochim. Acta 65 (2001) 3769–3778, https://doi.org/10.1016/S0016-7037(01)00655-X
[48] J. Schnaidt, M. Heinen, Z. Jusys, R.J. Behm, Oxidation of the partly oxidized ethylene glycol oxidation products glycolaldehyde, glyoxal, glycolic acid, glyoxylic acid, and oxalic acid on Pt electrodes: a combined ATR-FTIRS and DEMS spectro-electrochemical study, J. Phys. Chem. C. 117 (2013) 12689–12701, https://doi.org/10.1021/jp402986z
[49] C.S. Ewig, J.R.V. Wazer, Ab initio studies of molecular structures and energetics. 1 Base–catalyzed hydrolysis of simple formates and structurally related reactions, J. Am. Chem. Soc. 108 (1986) 4774–4783, https://doi.org/10.1021/ja00276a015
[50] S. Bohm, D. Antipova, J. Kuthan, Study of methanetriol decomposition mechanisms, Int. J. Quantum Chem. 60 (1996) 649–655, https://doi.org/10.1002/(SICI)1097-461X(1996)60:2<649::AID-QUA3>3.0.CO;2-X
[51] F. Bertini, N. Gorgas, B. Stöger, M. Peruzzini, L.F. Veiros, K. Kirchner, L. Gonsalvi, Efficient and mild carbon dioxide hydrogenation to formate catalyzed by Fe(II) hydrido carbonyl complexes bearing 2,6-(diaminopyridyl)diphosphine pincer ligands, ACS Catal. 6 (2016) 2889–2893, https://doi.org/10.1021/acscatal.6b00416
[52] X.J. Su, K.M. McCardle, L.Z. Chen, J.A. Panetier, J.W. Jurss, Robust and selective cobalt catalysts bearing redox-active bipyridyl-N-heterocyclic carbene frameworks for electrochemical CO_2 reduction in aqueous solutions, ACS Catal. 9 (2019) 7398–7408, https://doi.org/10.1021/acscatal.9b00708
[53] Y.F. Zhuge, G.L. Fan, Y.J. Lin, L. Yang, F. Li, A hybrid composite of hydroxyapatite and Ca-Al layered double hydroxide supported Au nanoparticles for highly efficient base-free aerobic oxidation of glucose, Dalton Trans. 48 (2019) 9161–9172, https://doi.org/10.1039/C9DT00985J
[54] N. Akiya, P.E. Savage, Roles of water for chemical reactions in high-temperature water, Chem. Rev. 102 (2002) 2725–2750, https://doi.org/10.1021/cr000668w
[55] Z.Y. Liu, E.W. Huang, I. Orozco, W.J. Liao, R.M. Palomino, N. Rui, T. Duchoň, S. Nemšák, D.C. Grinter, M. Mahapatra, P. Liu, J.A. Rodriguez, S.D. Senanayake, Water-promoted interfacial pathways in methane oxidation to methanol on a CeO_2-Cu_2O catalyst, Science 368 (2020) 513–517, https://doi.org/10.1126/science.aba5005
[56] Y.L. Zhang, Z. Shen, X.F. Zhou, M. Zhang, F.M. Jin, Solvent isotope effect and mechanism for the production of hydrogen and lactic acid from glycerol under hydrothermal alkaline conditions, Green. Chem. 14 (2012) 3285–3288, https://doi.org/10.1039/C2GC36153A
[57] E. Garcia Verdugo, Z. Liu, E. Ramirez, J. Garcia Serna, J. Fraga Dubreuil, J.R. Hyde, P.A. Hamley, M. Poliakoff, In situ generation of hydrogen for continuous hydrogenation reactions in high temperature water, Green. Chem. 8 (2006) 359–364, https://doi.org/10.1039/B515470G
[58] M. Grasemann, G. Laurenczy, Formic acid as a hydrogen source-recent developments and future trends, Energy Environ. Sci. 5 (2012) 8171–8181, https://doi.org/10.1039/C2EE21928J
[59] C. Fellay, P.J. Dyson, G. Laurenczy, A viable hydrogen-storage system based on selective formic acid decomposition with a ruthenium catalyst, Angew. Chem. Int. Ed. 47 (2008) 3966–3968, https://doi.org/10.1002/anie.200800320
[60] S. Kar, M. Rauch, G. Leitus, Y. Ben-David, D. Milstein, Highly efficient additive-free dehydrogenation of neat formic acid, Nat. Catal. 4 (2021) 193–201, https://doi.org/10.1038/s41929-021-00575-4
[61] X.G. Zhu, S.P. Long, D.R. Ort, What is the maximum efficiency with which photosynthesis can convert solar energy into biomass, Curr. Opin. Biotechnol. 19 (2008) 153–159, https://doi.org/10.1016/j.copbio.2008.02.004
[62] Long, S.P., Colon, A.M. Zhu, X.G. Meeting the global food demand of the future by engineering crop photosynthesis and yield potential. Cell 2015, 161, 56–66. 10.1016/j.cell.2015.03.019.